IS THE FOOTPRINT OF AN AFTERSHOCK SEQUENCE LARGER THAN WE THINK: A NEW VIEW FROM THE WELL RECORDED AFTERSHOCKS OF THE 2001 AND 2005 MAGNITUDE ∼5 ANZA, CALIFORNIA, EARTHQUAKES

Karen R. Felzer
U. S. Geological Survey
525 S. Wilson, Pasadena, CA 91106

Debi Kilb
Institute of Geophysics and Planetary Physicst
University of California, San Diego
La Jolla, CA 92093-0225

September 15, 2008

1 Abstract

It has been traditionally held that aftershocks occur within one to two mainshock fault lengths of the mainshock. Here we demonstrate that this perception has been shaped by the sensitivity of seismic networks. Much larger aftershock zones can be observed for the the well recorded 31 October 2001 M_W 5.02 and 12 June 2005 M_W 5.2 Anza sequences in southern California. These earthquakes occurred in the middle of the densely instrumented ANZA seismic network and thus were unusually well recorded. For the June 2005 event, aftershocks as small as M 0.0 could be observed stretching for at least 50 km along the San Jacinto Fault zone even though the mainshock fault was only $\sim$4.5 kilometers long. It was hypothesized by Agnew and Wyatt (2005) that an observed aseismic slipping patch was responsible for this extended aftershock sequence. An aseismic slipping patch would provide a spatially extended aftershock-triggering source, which would presumably slow the decay of aftershock density with distance, leading to a broader aftershock zone. Contrary to this, we find the decay of aftershock density with distance in both Anza sequences to be similar to that observed in other California aftershock sequences. This indicates that there is no need for additional mechanisms beyond typical seismic triggering. Our results suggest that with widespread dense instrumentation, aftershock sequences would routinely have footprints much larger than currently expected. Despite the large aftershock zone, however, we find that the probability that the 2005 Anza mainshock triggered the M 4.9 Yucaipa mainshock, which occurred 4.2 days later and 72 km away, to be only 14% $\pm$ 1%. This relatively low probability is a strong function of the 4.2 day delay between the two earthquakes. Had the Yucaipa earthquake occurred only 1 hour after the Anza earthquake, the probability of triggering would have been 89%.

Supplemental Material: http://eqinfo.ucsd.edu/$\sim$dkilb/BSSA_Felzer_Kilb.html

2 Introduction

The relationship between a mainshock and its aftershocks has been a topic of study for decades (Omori 1894; Benioff 1951; Utsu 1961; Scholz 1968; Nur and Booker 1972; Das and Scholz 1981; Dieterich 1994;

Toda et al. 1998; Kilb et al. 2000; Parsons 2005; Helmstetter and Shaw 2006; Hill 2008), yet many basic questions about the physics of aftershock triggering remain unresolved (Gomberg 2001). For example we do not know the underlying physics of how one earthquake triggers another, nor is there consensus on the distance extent between a typical aftershock and the triggering mainshock.

Until the early 1990's it was commonly believed that all triggered earthquakes occurred within a zone of 1 to 2 mainshock fault lengths from the mainshock hypocenter (Hough and Jones 1997). But in 1992 researchers discovered that the M_W 7.3 Landers, California, earthquake triggered seismicity well beyond this zone (Hill et al. 1993). Since then, a number of other $M \geq 7$ earthquakes (Brodsky et al. 2000; Glowacka et al. 2002; Prejean et al. 2004; West et al. 2005) as well as smaller M 2–4 mainshocks (Felzer and Brodsky 2006) have been shown to trigger earthquakes at distances as far as tens of fault lengths from the mainshock. These new observations have generated substantial controversy regarding whether distant triggered earthquakes are regular aftershocks – that is, generated by the same physical process as near field events – or represent a separate phenomena (Hough 2005; Steacy et al. 2005; Main 2006).

One convenient place to investigate the size of the regular aftershock zone is in the Anza, California, region along the San Jacinto fault. The Anza region contains a dense seismic network operated by the Scripps Institution of Oceanography (www.eqinfo.ucsd.edu), and this region has a substantially lower seismic attenuation than other densely instrumented regions in California, such as Parkfield. The benefit of data recorded in regions of low attenuation is that a stronger signal reaches the surface, making interpretation of seismograms easier. Anza is characterized by a very competent granitic geology, and despite a number of shallow regions of low Q, Hough et al. (1988) found an average Q of $\sim$1000 at seismogenic depths for P and S waves. At Parkfield, on the other hand, Abercrombie (2000) found an average Q of 200 on the southwest side of the fault, an average Q of 100 on the northeast, and a thick layer of lower Q (varying from around 20 to 55) near the surface – a layer so thick, in fact, that the Parkfield borehole stations are deployed within it, not below it.

M_W 5.02 and M_W 5.2 mainshocks occurred in the Anza region in 2001 and 2005, respectively (Figure 1). For both mainshocks a large number of small aftershocks were recorded, and relatively large aftershock zones could be seen; in the case of the 2005 mainshock, aftershocks extended at least 50 km along the San Jacinto Fault zone (Figure 2). From the empirical magnitude/fault length relationships of Wells and Coppersmith (1995) we estimate that the M_W 5.2 2005 mainshock was only $\sim$4.5 kilometers long. The

observed 50 km long aftershock zone was viewed by the seismological community as an uncommon occurrence, possibly caused by an observed aseismic slip patch that presumably encompassed the region of aftershock activity (Agnew and Wyatt 2005). Although the recording of this sequence is unprecedented, the data are not sufficient to determine the exact position or size of this aseismic slipping patch. It is also not known whether large patches of aseismic slip routinely accompany earthquakes because the strainmeter instrumentation needed to record these phenomena is not commonly used, and was not even operational during the 2001 Anza mainshock/aftershock sequence.

In this paper, we demonstrate that the large extent of the 2005 Anza aftershock sequence was likely not caused by an unusual event because the density of aftershocks decayed with distance from the mainshock fault at the same rate as observed elsewhere in California. This typical decay was also seen after the 2001 sequence. Furthermore, both Anza sequences agree well visually with simulations of normal aftershock sequences with low earthquake catalog completeness levels. This suggests that if we could routinely catalog many small aftershocks, most aftershock zones would appear to cover a wide area. We also demonstrate that despite the large aftershock zones of the Anza earthquakes the M_W 4.9 earthquake near the town of Yucaipa, which occurred 4 days after and 72 km away from the 2005 Anza epicenter, was probably not an aftershock of the 2005 Anza earthquake.

3 Data

We examine the mainshock and aftershock sequences of the 31 October, 2001 M_W 5.02 Anza earthquake (33.52°; -116.50°; depth 18) and 12 June 2005 Anza M_W 5.2 earthquake (33.53°, -116.58°, depth 14.1 km). We also look at the relationship between the 2005 Anza mainshock and the M_W 4.9 Yucaipa earthquake (33.99°, -117.03°, depth 17 km) that occurred 4 days later. The two Anza sequences occurred directly under the ANZA seismic network (see Data and Resources Section), which spans the San Jacinto fault zone in southern California (Berger et al. 1984; Vernon 1989). Rarely are continuous waveform data of such high quality available. Within our local study region (32.0°$<$ lat $<$34.5°; -117.90°$<$ lon$<$-115.60°; depth$<$ 25 km) the Anza network catalog contains 499 and 1615 earthquakes, in total, in the initial two days for the 2001 and 2005 sequences, respectively, and clearly captured many more small earthquakes than was possible just a decade ago (Figure 3).

We augment the 2005 ANZA Network data with data from the Southern California Seismic Network (SCSN) catalog (see Data and Resources section). We quantify the degree of variability between the ANZA and SCSN catalogs by comparing 881 earthquakes common to both catalogs (350 in the 2001 sequence and 531 in the 2005 sequence). The ANZA network reports that the earthquakes are deeper on average by approximately 2-3 km. The ANZA and SCSN catalogs also differ on the magnitudes of the earthquakes; the median difference between the assigned magnitudes is about 0.5$\pm$0.3, with earthquakes in the SCSN catalog on average $\sim$0.5 magnitude units higher than the corresponding earthquake in the ANZA Network catalog, although with significant scatter (Figure 4). The discrepancy in magnitude likely arises from a combination of different station corrections used by the two networks and the fact that the primary footprint of the ANZA network spans a relatively small area (Frank Vernon, personal communication). These data have hypocentral distances $<$20 km, and short hypocentral distances have been shown to bias M_L magnitudes downwards (Bakun and Joyner 1984).

4 Method

4.1 Investigating the large spatial extent of the Anza aftershock sequences

The first question we address is whether the spatially extended 2005 Anza aftershock sequence comprises normal, seismically triggered aftershocks or, alternatively, aftershocks triggered by a zone of extended aseismic slip. We do this by measuring how quickly the density of triggered aftershocks decays with distance from the mainshock fault plane and visually comparing the sequence with simulated ones that follow typical aftershock statistics. Included in our simulation is a low aftershock magnitude detection threshold comparable to the one attained by the ANZA network. To assess our results, we determine if the Anza aftershock density decays with distance like normal sequences, indicating no triggering by aseismic slip is required, or if the density decays more slowly, suggesting triggering by an aseismic slip patch is more plausible. Using this approach we are assuming that aseismic slip patches do not routinely accompany M 5 earthquakes.

Felzer and Brodsky (2006) found that for southern California aftershock sequences aftershock density decays on average with distance, r, as

$$\rho(r) = cr^{-1.37} \tag{1}$$

where r is the shortest distance, in 3D, between the aftershock and the mainshock fault plane, c is a constant

that varies with mainshock magnitude, minimum aftershock magnitude, and elapsed time, and $\rho(r)$ is linear density, which measures the number of aftershocks per kilometer. We compare the results from Equation 1 with data from the Anza Seismic Network and SCSN and determine if they differ using three different tests.

First, we count the number of earthquakes in annuli around the 2001 and 2005 Anza mainshocks and compare these values with predictions from Equation 1. Second, we measure and fit the linear density of the Anza aftershocks as a function of distance. The linear density is measured with the nearest neighbor method (Silverman 1986), which is a non-parametric measurement. The aftershocks are first plotted on a line as a function of their distance, r, to the mainshock fault (Figure 5). Consecutive points on the line are then placed into groups, with the same number of aftershocks in each group. The density at the center of each group, at distance r_c from the mainshock, is given by

$$\rho(r_c) = \frac{k}{r_n} \tag{2}$$

where k is equal to the number of points in each group and r_n is the length of the nth group, as illustrated in Figure 5. We use $k = 1$, which maximizes the data scatter but gives us the lowest parameter fitting error because smoothing, and information loss, is minimized. The azimuth of the aftershocks is not used in the calculation of linear density and does not affect the results.

Finally, we do a visual comparison of the Anza aftershock sequences with simulations made with the ETAS aftershock model (Ogata 1988; Felzer et al. 2002; Helmstetter et al. 2006). The ETAS model simulates aftershocks using robust empirical laws of aftershock behavior. The laws we use are the modified Omori law for aftershock rate decay with time (Utsu 1961) (see Appendix A for the calculation of our modified Omori law parameters), the Gutenberg-Richter magnitude-frequency relationship (Gutenberg and Richter 1944), with a b parameter of 1.0, and the Felzer-Brodsky relationship (Felzer and Brodsky 2006) (Equation 1) for the decay of aftershock density with distance. The largest aftershock we allow in the simulation is M 3.65, which is the magnitude of the largest earthquake in the data catalog for this region. Using the maximum magnitude in the real data for the simulation is important because the overall productivity of the aftershock sequence will vary with the largest aftershock magnitude, and the apparent spatial extent of the aftershock sequence, in turn, varies with this overall productivity.

We inspect aftershocks in the first two days of the aftershock sequences for both the 2001 and 2005

mainshocks because this time period is short enough to minimize the inclusion of unrelated background earthquakes while being long enough to provide a reasonable amount of aftershock data. Because we use data down to small magnitudes and over a large area, the background earthquakes can accumulate quickly, so a short time period for measuring aftershocks is essential.

An important issue for all of our tests is catalog completeness. When we measure the decay of aftershock density with distance we do not need our catalog to be 100% complete above our chosen magnitude threshold, but we do need the level of completeness to be consistent over the distance range inspected. We test for completeness consistency by measuring the correlation coefficient between distance from the mainshock and the magnitudes of aftershocks in the ANZA catalog. Limiting our catalog to $M \geq 0.5$ earthquakes we find no significant correlation for distances ranging up to 40 km. Beyond 40 km, the correlation becomes positive, presumably because we are leaving the core of the Anza network and completeness is decreasing. For our quantitative measurements of aftershock density as a function of mainshock-aftershock distance we therefore limit our data to $M \geq 0.5$ earthquakes located at $\leq$ 40 km or less from the mainshock fault plane.

For our qualitative comparison between the Anza 2001 and 2005 aftershock sequences and the ETAS simulation of these sequences we need an estimate of the absolute completeness threshold, which will serve as the minimum magnitude for our simulations. Determining the absolute completeness threshold is a very difficult task. The most comprehensive method for solving for completeness over a region is to invert for the detection sensitivity of nearby seismic stations and then forward-solve for the completeness at each point given its distance from each station (Schorlemmer et al. 2006). This method is complex, however, and our current problem does not require such an accurate solution. So instead, we estimate the completeness threshold from a magnitude frequency plot of the data, determining at what magnitude the number of earthquakes falls below that predicted by the Gutenberg-Richter magnitude frequency relationship (Gutenberg and Richter 1944). This method yields completeness thresholds of M $\sim$1.5 and M $\sim$1.0 for the 2001 Anza sequence in the SCSN catalog and Anza network catalogs, respectively. For the 2005 Anza sequence the fall off occurs at M $\sim$1.0 in the SCSN catalog (Figure 6). A fall off is not readily apparent in the Anza network catalog for magnitudes down to M 0. Since we previously found evidence of the catalog becoming incomplete below M 0.5 near the edges of the Anza region, we assign a threshold of M 0.5 for this catalog.

Another concern with our data is potential inaccuracy in the calculated distances between the aftershocks and the mainshock fault plane in the near field, caused by errors in aftershock locations and our assumption

that the Anza 2001 and 2005 mainshocks ruptured perfectly planar faults. Most large earthquake rupture planes have complexities, such as irregular fault surfaces, step overs, and bends. A study by Walker et al. (2005), found aftershocks in the 2001 Anza sequence to be quite heterogeneous (41% strike slip, 41% thrust, and 18% normal based on earthquakes in the first month of the sequence), suggesting that this mainshock fault surface was particularly complex. To avoid this near field complexity, which prevents us from knowing exactly where the mainshock fault is located, we do not use aftershocks that are closer than 4 km to the modeled position of the mainshock fault plane in our quantitative analysis. The 4 km limit is approximately the average fault length of our mainshocks.

Our distance, time, and magnitude cutoff requirements as specified above, results in a total of 68 aftershocks for quantitative analysis of the Anza 2001 earthquake using the ANZA catalog, a total of 49 aftershocks for analysis of Anza 2005 from the ANZA catalog, and a total of 55 aftershocks for our quantitative analysis of the 2005 mainshock using the SCSN catalog. For the qualitative comparison of map views of the data with map views of the simulations, for which we cover distances from 0 to 100 km and use different magnitude cutoffs as specified above, we have 198 $M \geq 1.0$ aftershocks in the first two days of the 2001 Anza network catalog and 387 $M \geq 0.5$ aftershocks in the first two days of the 2005 Anza network catalog.

4.2 Investigating whether the Yucaipa earthquake was triggered by the 2005 Anza mainshock

Given the proximity in space and time between the 2005 Anza and Yucaipa earthquakes (4.2 days and 72 km), and the broad region covered by the 2005 Anza aftershocks, we investigate the probability that the Anza mainshock triggered the earthquake in Yucaipa. A precise solution would require knowing the seismicity rate in the Yucaipa region at the time of the Yucaipa earthquake had the Anza mainshock not occurred. Answering this question requires accurate compilation of the local background rate plus the aftershock sequences of all earthquakes that could possibly affect the region at that time. Even if we could do this calculation with high precision we would still be left with the vexing question as to what the appropriate spatial extent is of the "Yucaipa source region", ie., over what region should this background rate be calculated? Because it is currently impossible to answer these questions without large uncertainties, we instead compute a general empirical solution of the probability that a M 5–6 mainshock in California will trigger

an $M \geq 4$ earthquake occurring four days after and more than 72 km away. This general calculation also has the benefit of being applicable to other triggering scenarios. We use M 4.0 as our cutoff, rather than M 4.9, because this lower threshold increases our chances of actually capturing distant aftershock triggering by nearly tenfold. Repeated study has shown that aftershocks follow the Gutenberg-Richter mgnitude frequency relationship, and thus if $M \geq 4$ aftershocks occur then so will $M \geq 4.9$, just at roughly one tenth the rate (Felzer et al. 2004).

To compute the empirical solution we first select all M 5 – 6 earthquakes from the SCSN and the Advanced National Seismic System (ANSS) catalogs occurring in California from 1984-2006 that were not preceded within $T1$ days by a larger earthquake anywhere in the state. This exclusion is done so that the resulting catalog will contain earthquakes that are much more likely to be triggered by the selected mainshocks than by some larger earthquake. We next chose an earthquake triggering inspection time, $T2$, which spans from the mainshock event to $T2$ days latter. Finally, the "background" seismicity rate is estimated from seismicity occurring from time $-T3$ to -0.5 days before the mainshocks. Seismicity occurring in the last 0.5 days before the mainshock is not included because the seismicity rate can be strongly increased by foreshock activity right before the mainshocks. Because it is impossible to entirely remove aftershocks of foreshocks from the data, technically the triggered earthquakes that we observe could have been triggered by either the target mainshocks or aftershocks that preceded them within 12 hours.

The year 1984 is chosen as a starting point for this exercise because after this date a good, statewide, instrumental earthquake catalog exists. We find that the background rate measured for a particular choice of $T1$, or the exclusion time after larger earthquakes, is fairly stable for choices of $T3$ (the time at which we start measuring background earthquakes) ranging from 25 to about 75 days (unless $T1 < 75$, in which case the range of stability is narrower). Values of $T3$ shorter or longer than this result in higher background rates; in the first case because the rate becomes too dominated by foreshock activity, and in the second case because we start capturing too many aftershocks of the larger mainshocks that occurred prior to $T1$. The background rate does vary by a factor of about 2 when $T1$ is varied between 50 and 500 days. For $T1 = 50$ days, for example, and $T3 = 25$ days, we measure a background rate at > 72 km of 0.035 $M \geq 4$ earthquakes/day, whereas $T1 = 400$ days gives 0.02 $M \geq 4.0$ earthquakes/day. The reason for the decrease in the "background" rate with increased $T1$ is that larger values of $T1$ mean more time since the last larger earthquakes, and hence fewer residual aftershocks of these earthquakes are occurring. The 2005

Anza mainshock occurred 257 days after the last $M \geq 5.2$ earthquake in California. Setting $T1 = 257$ days and allowing $T3$ to vary from 25 to 75 days we recover a mean background rate of 0.0285 $M \geq 4$ earthquakes/day with a 98% confidence range from 0.0255 to 0.0293 $M \geq 4$ earthquakes/day.

Estimating the percentage of triggered earthquakes within the triggering inspection time, and hence the probability that any particular observed earthquake, such as the Yucaipa earthquake, was triggered by an earthquake in the mainshock data set, is done by simply subtracting the calculated background earthquake rate from the total rate observed in the triggering inspection time and then dividing by this total. That is,

$$P = (Tot - B)/Tot \tag{3}$$

where $P =$ the percentage triggered, Tot is the total number of earthquakes observed, and B is the calculated background rate. As demonstrated above the value of B is generally quite stable if we use inspection time periods of 25 to 75 days and a constant value of $T1$. Estimation of Tot, however, is affected by two sources of error. The first is the random Poissonian variation in the number of background earthquakes that will occur during the triggering inspection time, even if the average background rate is stable. The other source of error is the limited number of mainshocks, meaning that the average triggering rate observed for the mainshocks available might not be the true population average. Both of these errors are considered in the calculations below.

5 Results

5.1 Aftershocks of the Anza earthquakes

We find that aftershock density as a function of distance from the mainshock for both Anza mainshocks follows an inverse power law decay, with decay rates a bit steeper than the California average (Figure 7). This indicates that the spatial distribution of Anza aftershocks are similar to those observed in other, assumed typical, aftershock sequences. We conclude that there is no excess aftershock activity at distance that would indicate the need for an unusual triggering mechanisms such as an aseismic slip patch.

We next confirm that the decay of aftershock density with distance for the Anza sequences is normal by counting the number of earthquakes in different distance annuli around the mainshocks. The mean number of earthquakes that we expect in each annulus is given by Equation 1 where the constant c in that equation

is determined from the total number of aftershocks observed in the annulus stretching from 4 to 10 km. The 98% range on the number of earthquakes that we expect to observe in each annulus, given data set size, is calculated via 500 ETAS simulations. We find that the 16-22 km distance bin for the 2001 sequence has fewer aftershocks than expected, falling below the 98% confidence interval of the model, but the number of aftershocks within the rest of the annuli for both the 2001 and 2005 sequences are within the expected ranges (Figure 9).

As a final test, we qualitatively compare map views of the 2001 and 2005 Anza aftershock sequences with our ETAS simulated aftershock sequences. All simulations compare favorably with the data. This demonstrates that when aftershock sequences following the statistical empirical laws modeled by the ETAS simulation are visualized down to aftershocks as small as M 0.5 or M 1, the spatial distribution appears much larger than if only viewing aftershocks $M \geq 2.0$, which is the more common completeness threshold in California (Figure 8).

5.2 Triggering of the Yucaipa Earthquake

We next investigate if the 2005 Anza mainshock triggered the 2005 Yucaipa earthquake (the time and space separation between these two events was 4.2 days and 72 km, respectively). Over the last 60 years there has been an average of 3.6 $M \geq 4.9$ earthquakes recorded per year in our southern California study region (including all aftershock sequences). Thus if we were to assume a stationary seismicity rate, the probability of randomly having two $M \geq 4.9$ earthquakes separated by 4 days or less is only $\sim$3%.

We estimate, as described in Equation 3, the probability that the Yucaipa earthquake was triggered by the Anza earthquake by looking at triggering, at distances up to 72 km, of $M \geq 4$ earthquakes surrounding M 5–6 mainshocks. Our catalog, generated by the Working Group on California Earthquake Probabilities (WGCEP) (Felzer and Cao 2008), includes data from California and regions with 100 km of California, which occurred between 1984-2006. We assume the 72 km distance between the Anza and Yucaipa mainshocks has minimal (i.e., < 2 km) and so no other distance ranges are tested.

The first important result is that we can observe clear triggering ($> 98\%$ confidence) by the M 5–6 mainshocks at distances of > 72 km for short time periods after the mainshocks. For a larger earthquake exclusion period, $T1$, of 200 days, and an inspection window, T2, of 0 to 0.5 days, for example, Equation 3 gives that 92% of the earthquakes at ≥ 72 km are triggered by the mainshocks, with a 98% confidence

range of 50% to 100%. The large error bars result from the small number of earthquakes available for the calculation; with the stated parameters we have only 28 mainshocks and a total of only 4 observed $M \geq 4$ earthquakes at > 72 km and 0 to 0.5 days, 0 to 2 of which may be background earthquakes. The important point is that we can be highly confident that some triggering is occurring, even though 72 km is more than ~ 5 times longer than the fault length of our largest mainshock. If we increase $T1$ to 400 days, lowering the background rate, we recover that 97% of the earthquakes at > 72 km and 0-0.5 days are triggered by our mainshocks, with a 98% error range from 66% to 100%. The occurrence of some amount of triggering at > 72 km and 0-0.5 days can be verified at over 98% confidence for all values of $T1$ between 50 and 500 days; for $T1$ less than 50 days there is too much interference from aftershocks of larger earthquakes to see a clear triggering signal, and for $T1$ greater than 500 days there are simply too few qualifying mainshocks. The existence of triggering at > 72 km can also be seen at 98% confidence at 0.25 to 0.75 days for values of $T1$ between 250 and 500; for $T1 = 250$ days, for example, we have that 90% of the earthquakes are triggered with a 98% confidence range from 50% to 100%.

Triggering cannot be verified with high confidence for an inspection time, $T2$, of 0.5 to 1.0 days, or any later time period, however, regardless of the choice made for $T1$. This may be because the triggering stops, in which case the Yucaipa earthquake could not have been triggered by the 2005 Anza mainshock. Alternatively triggering may continue but at such a low rate that it cannot be seen above the background rate at high statistical confidence in our limited sample. If, for example, the background rate is such that we expect between $B1$ and $B2$ background earthquakes to occur in the 0.5 to 1.0 day time period, then in order to observe statistically significant triggering we need the total number of earthquakes observed to be $> B2$. If we can show that the rate of triggering is such that $> B2$ total earthquakes may be reliably expected, yet triggering is not observed, then we may conclude that triggering at > 72 km ceases after ~ 0.5 days. On the other hand if we find that the the number of earthquakes triggered should be $\leq (B2 - B1)$ the majority of the time then it is reasonable to assume that the triggering continues, as it continues past 0.5 days at closer distances, but that the signal to noise ratio is low.

To determine if the total number of earthquakes should be $> B2$ we need to find what the aftershock rate should be at 72 km and 0.5 to 1 days, which we do by extrapolating the triggering rate observed at 0.25-0.75

days using Omori's law for aftershock decay (Omori 1894),

$$r = Kt^{-p} \tag{4}$$

where r is the aftershock rate, t is time, and K and p are constants. Here we do not include the c value used in the modified Omori law ($K(t+c)^{-p}$) (Utsu 1961) because the c value is generally small ($<<$ 1 day) and thus unimportant given that we are starting at 0.25 days. We also do not have enough data to solve for the value of p, so we set it at the average California value of 1.08 found by Reasenberg and Jones (1989). We then find the full range of possible values of K by setting $T1$, or the exclusion period for larger earthquakes, at varying values between 50 and 500. Accounting for Poissonian and measurement error, we obtain a range of K from 0.0121 to 0.0279, where K is calculated for a mainshock magnitude average of M 5.4 and the production of $M \geq 4$ aftershocks per day.

Now returning to the data set, if we set $T1$ to 400 days, giving us the lowest background rate of 0.02 $M \geq 4$ earthquakes/day/mainshock, then we have 11 mainshocks. This gives that from 0.5 to 1.0 days we expect a total background rate of $(0.02/2) \times 11$ = 0.11 background earthquakes, or an actual earthquake count of 0 to 1 98% of the time ($B1 = 0$, $B2 = 1$). This means that we need to observe 2 or more earthquakes to clearly ascertain triggering. Assuming the highest value of K (0.0279) we expect these mainshocks to produce 0.0015 $M \geq 4$ aftershocks/mainshock over the time period 0.5 - 1.0 days, or a total of (0.0015*11) = 0.0165 aftershocks, which translates to a single observed aftershock only $\sim 1.6\%$ of the time, and 2 aftershocks only $\sim 0.01\%$ of the time. Thus with this data set we are unlikely to observe statistically clear triggering at 0.5 - 1 days, even if the triggering process is still occurring. We next try setting $T1 = 50$, increasing our data set to 67 mainshocks and the background rate to 0.035 $M \geq 4$ earthquakes/day/mainshock. In this case the expected number of background earthquakes over the observation period is 0 to 4, and the expected number of aftershocks is 0 (90% of the time) to 1 (9.95% of the time). Running 1000 Monte Carlo trials indicates that we can only expect a total of ≥ 5 earthquakes to occur 0.1% of the time – so it is no surprise that we do not observe significant triggering in our sample.

On the basis of the above calculations, if we assume that triggering at > 0.5 days and > 72 km does in fact continue, just at rates too small to be observed above background in our limited data set, then the 2005 Anza earthquake may have triggered the earthquake at Yucaipa 4.2 days later, and the values of K and

the background seismicity rate solved for above may be used to solve for the probability that this triggering did in fact occur. First we note that the K value solved for above is referenced to M 5.4 mainshocks; to correct this to the M 5.2 magnitude of the Anza mainshock we multiply by $10^{5.4-5.2} = 10^{-0.2}$ (Felzer et al. 2004). We also use the lowest value of K from the range given above, since it is the closest to the value found for the majority of choices of $T1$. This gives us a triggering rate of 0.0045 $M \geq 4.0$ earthquakes per day at 4.2 days and > 72 km. Substituting this into Equation 3 and using the background seismicity rate for Anza given above (e.g. for $T1 = 257$ days) gives a $14\% \pm 1\%$ probability (98% confidence interval) that the Yucaipa earthquake was triggered by the Anza mainshock. Note that if the 2005 Anza and Yucaipa earthquakes had a smaller temporal separation, the probability of a triggering relationship would have been much higher. For a one hour separation, for example, the probability of triggering would have been about 89%, and for a 12 hour (half day) separation, the probability would be about 36%.

6 Discussion

The size of an aftershock zone can appear misleadingly small if substantial effort is not taken to catalog small magnitude aftershocks using data recorded by robust seismic networks close to the source region. Our analysis of the M_w 5.2 Anza 2005 aftershock sequence illustrates how strongly our perception of the spatial extent of an aftershock sequences is shaped by monitoring. Traditionally, instrumentation and routine processing in southern California limit the detection of aftershocks to those larger than approximately M 2. For large mainshocks, even many M 2 aftershocks cannot be initially observed (Enescu et al. 2007; Kilb et al. 2007). If only the few $M \geq 2$ aftershocks of the 2001 and 2005 Anza mainshocks had been observed, these sequences would have appeared to cover a much smaller area than the area revealed when $M \geq 1.0$ or $M \geq 0.5$ aftershocks are included (Figure 2). In fact, the clearly clustered area of $M \geq 2$ aftershocks are within the 1 to 2 mainshock fault length radii region previously assumed to be the limits of an aftershock zone. The dense instrumentation, careful processing, and low attenuation at Anza provides the unique opportunity to observe a much larger spatial extent of aftershocks (see supplemental movies http://eqinfo.ucsd.edu/$\sim$dkilb/BSSA_Felzer_Kilb.html). These observations clearly support the idea that the spatial footprint of aftershock zones can extend out to tens of kilometers, even after small or moderate mainshocks.

We emphasize that our results do not indicate that aftershocks routinely occur out to ten fault lengths whatever the magnitude of the mainshock, but rather that they can occur out to at least 50 km after moderate earthquakes. This result is consistent with others in the literature, for example Felzer and Brodsky (2006) demonstrated that aftershock zone size does not in fact scale with mainshock fault length, and that the perception that it does simply results because larger mainshocks have more aftershocks, and usually only the larger aftershocks (e.g. a small percentage of the total) can be identified. They conclude that for mainshock magnitudes of at least M 2-6 aftershocks occur out to at least 50 km independent of the mainshock magnitude. This result is consistent with the 50 km spatial extent of the Anza 2005 sequence found in this study.

Guided by observational limitations, aftershock zones containing "normal" aftershocks (presumably all triggered by the same physical mechanism), were previously expected to be limited in size because it was assumed that the aftershocks were triggered by static stress changes, which decay very quickly with distance. A number of recent papers, however, have found evidence that most early (and quite possibly later) aftershocks, at all distances, are likely triggered by the more slowly decaying dynamic stress changes (Kilb et al. 2000; Parsons 2002; Gomberg et al. 2003; Prejean et al. 2004; Felzer and Brodsky 2006; Mallman and Zoback 2007). Perhaps one of the most convincing studies is the recent demonstration by Pollitz and Johnston (2006) that seismic events occurring near San Juan Bautista produced at least 10 to 20 times more aftershocks than nearby aseismic episodes with similar seismic moment release.

If most aftershocks are triggered by dynamic stress changes, and if the triggering of some aftershocks at far distances is a standard occurrence, even for smaller mainshocks, then there could be a causal relationship when two earthquakes occur relatively close in time to each other, even if they are separated by a significant distance. In the case of the 2005 Anza-Yucaipa pair, we find a 14% $\pm 1\%$ probability that Yucaipa was triggered by the Anza mainshock, which is not very large, but non-negligible. Due to the rapid inverse power law decay of aftershock rate, the probability of triggering would have increased substantially if the two earthquakes had been closer together in time (i.e., if the time separation was 1 hour the probability of a triggering relationship would have been about 89%). These numbers, and the parameters solved for to calculate them, provide a general basis to estimate the probability of a triggering relationship between two California earthquakes.

7 Conclusions

Aftershocks of the 2005 M_W 5.2 Anza earthquakes extended along ∼50 km of the San Jacinto fault – a distance of over ten times the ∼ 4.5 km fault lengths of the mainshock. This was viewed as unusual because it has been traditionally held that the normal aftershock zone extends only 1 to 2 fault lengths from the mainshock. Here, we have demonstrated that the common perception of aftershock zone size is highly colored by the sensitivity of the seismic network. At Anza, as a result of dense instrumentation and low attenuation, many aftershocks as small as M 0.5 and M 0.0 could be detected, and we have shown that this higher detection is sufficient to explain the extended appearance of the aftershock zone for the 2005 earthquake and also for an $M_W 5.02$ earthquake that occurred at Anza in 2001. Models of typical California aftershock sequences with aftershock detection as good as that at Anza appear similar to the Anza sequences, and the decay of aftershock density with distance from the mainshock fault planes at Anza is as rapid as for other mainshocks in California. These data support the hypothesis that aftershocks routinely occur over distances much greater than two mainshock fault lengths. The reason this extended aftershock zone is a relatively new idea is because it requires a sophisticated network and data cataloging team to capture and catalog the small earthquakes that make up most of the extended aftershock zones.

We also calculate the probability that the 2005 Anza M_W 5.2 mainshock triggered the 2005 Yucaipa M_W 4.9 earthquake, which occurred 4 days later at a distance of 72 km. Based on a 60 year data catalog for the region, the long term probability of randomly having two magnitude ∼4.9 earthquakes separated by 4 days or less is only ∼3 %. To estimate the probability that the Anza earthquake triggered the Yucaipa earthquake we look at the triggering of $M \geq 4$ earthquakes at similar distances and times using 67 M 5–6 California earthquakes. We find triggering occurring (increase of observed seismicity over the background rate at $> 98\%$ confidence) at distances $\geq$ 72 km out to times of 0.25 - 0.75 days after the mainshocks. At later times the triggering rate becomes too low to detect aftershocks above the background rate with high confidence. If we assume that triggering is still occurring nonetheless, and use Omori's law to extrapolate aftershock rates observed earlier to the 4.2 day separation between the Anza and Yucaipa events, we estimate a 14% $\pm 1\%$ probability that the Yucaipa event was triggered by the Anza mainshock.

8 Data and Resources

Earthquake catalog data was obtained from the Southern California Seismic Network (SCSN) and by personal communication with members from the Anza seismic network team (http://eqinfo.ucsd.edu/deployments/anza/index.ph last accessed June 28, 2007). SCSN data was obtained from the web page http://www.data.scec.org/catalog_search/date_mag_ and was last accessed June 9, 2006. We also use $M \geq 4$ 1984-2006 catalog data from the Working Group on California Earthquake Probabilities catalog (Felzer and Cao 2008).

Acknowledgements We thank J. Hardebeck and S. Hough for USGS internal reviews and thorough and thoughtful comments, and A. and L. Felzer for editing and assistance. Funding for D. Kilb was provided by the Blasker-Rose-Miah Fund, which is part of the science and technology grants from the San Diego Foundation. We are grateful to those associated with the collection, analyses and cataloging of the ANZA seismic network data and the Southern California Seismic Network data, without these data this work would not have been possible.

Appendix A: Solving for southern California direct modified Omori law parameters

One of the important components of our ETAS simulations is the modified Omori law (Utsu 1961), which gives the aftershock rate as a function of time. It has been shown that mainshock and aftershock magnitude may be incorporated into the equation and the law written as aftershock rate, R, given by:

$$R = k10^{(M_{main}-M_{aft})}(t+c).^{-p}, \tag{5}$$

(Felzer et al. 2002) where M_{main} is mainshock magnitude, M_{aft} is the magnitude of the smallest aftershock counted, and k, c, and p are constants. These constants are often used to describe the activity of the entire aftershock sequence – that is the compilation of direct and secondary triggers. In ETAS modeling, however, the direct versions of these parameters must be used – that is, the parameters which describe the activity level, with time, of direct aftershock sequences only. The full aftershock sequences are then naturally

formed as the direct aftershock sequence of each earthquake and the direct aftershock sequence of each of its aftershocks is simulated. Unfortunately, solving for the direct Omori law parameters is much more difficult than solving for parameters that describe full aftershock sequences.

To solve for the direct Omori law parameters for the ETAS simulation, we first need to make a distinction between the magnitudes M_{min} and M_{minS}. M_{min} is the true, but unknown, magnitude of the smallest earthquake in the system that produces aftershocks. M_{minS} is the smallest magnitude used to produce aftershocks in the ETAS simulation. A decrease in M_{minS} results in more accurate simulations, but the number of required calculations increases exponentially.

For our simulations we use $M_{minS} = 0.5$ when modeling aftershocks of the Anza mainshocks. The long term direct p value does not vary with M_{minS} (Sornette and Sornette 1999) and so we use the value of 1.34, solved for by Felzer et al. (2003). Since k and c, on the other hand, increase with M_{minS}, we start with $k = 0.0053$ and $c = 0.085$, which were solved for by Felzer et al. (2003) for $M_{minS} = 0$, and then increase these parameters incrementally until 100 thirty-day ETAS simulations for a M 6.0 mainshock produce on average about $10^{M_{main}-1.2-M_{minS}}$ aftershocks, which was derived from Båth's Law (Båth 1965; Richter 1958) see Felzer et al. (2002) and Helmstetter and Sornette (2003).

We further adjust k and c to fit our observation that southern California $M \geq 5.5$ earthquakes (in our 1984-2006 data base) have approximately 0.12 as many aftershocks from days 10 - 30 after the mainshock as from days 0 to 10. We also match the aftershock rates in the first two days, and the first five days, of the aftershock sequences of 62 M 4.7 - 5.7 southern California mainshocks occurring from 1984 through 2006. This mainshock magnitude range was chosen to span the magnitude of the 2005 M 5.2 Anza earthquake. The M 4.7 - 5.7 mainshocks chosen comprise all of the earthquakes in this magnitude range that occurred at least one year after and/or four fault lengths away from any larger earthquakes, thus ensuring that their observed early aftershocks are primarily their own and not part of a larger aftershock sequence. We express aftershock rates in terms of the number of aftershocks with magnitudes larger than or equal to their mainshock magnitude over a specified time period. We thus measure an average rate of 0.043 ± 0.036 mainshock/aftershocks over the first two days of the sequences, where error is given at the 98% confidence level solved from 500 bootstraps of the data, and a rate of 0.055 ± 0.03 mainshock/aftershocks over the first 5 days. In comparison, when we calculate ETAS simulations for the aftershock sequence of an M 5.2 mainshock with our final parameters for $M_{minS} = 0.5$ (Table 1) we recover a two day aftershock rate of

0.0426 ± 0.0006 aftershocks/mainshock (1000 simulations run, 500 bootstraps used to obtain 98% confidence error), and a 5 day total of 0.0532 ± 0.0008 mainshock/aftershocks. Thus, modeled and observed aftershock rates compare favorably.

References

Abercrombie, R. E. (2000). Crustal attenuation and site effects at Parkfield, California. *J. Geophys. Res. 105*, 6277–6286.

Agnew, D. and F. Wyatt (2005). Possible triggered aseismic slip on the san jacinto fault. In *Southern California Earthquake Center Annual Meeting*.

Bakun, W. H. and W. B. Joyner (1984). The M_L scale in central California. *Bull. Seis. Soc. Am. 74*, 1827–1843.

Båth, M. (1965). Lateral inhomogeneities in the upper mantle. *Tectonophysics 2*, 483–514.

Benioff, H. (1951). Earthquakes and rock creep: Part I: Creep characteristics of rocks and the origin of aftershocks. *Bull. Seis. Soc. Am. 41*, 31–62.

Berger, J. L., L. M. Baker, J. N. Brune, J. B. Fletcher, T. C. Hanks, and F. L. V. III (1984). The Anza array: A high dynamic range, broadband, digitally radio-telemetered seismic array. *Bull. Seis. Soc. Am. 74*, 1469–1481.

Brodsky, E. E., V. Karakostas, and H. Kanamori (2000). A new observation of dynamically triggered regional seismicity: earthquakes in greece following the August, 1999 Izmit, Turkey earthquake. *Geophys. Res. Let. 27*, 2741–2744.

Das, S. and C. H. Scholz (1981). Off-fault aftershocks caused by shear stress increase? *Bull. Seis. Soc. Am. 71*, 1669–1675.

Dieterich, J. A. (1994). Constitutive law for the rate of earthquake production and its application to earthquake clustering. *J. Geophys. Res. 99*, 2601–2618.

Enescu, B., J. Mori, and M. Miyazawa (2007). Quantifying early aftershock activity of the 2004 mid-Niigata Prefecture earthquake. *J. Geophys. Res. 112*, doi:10.1029/2006JB004629.

Felzer, K. R., R. E. Abercrombie, and Göran Ekström (2003). Secondary aftershocks and their importance for aftershock prediction. *Bull. Seis. Soc. Am. 93*, 1433–1448.

Felzer, K. R., R. E. Abercrombie, and Göran Ekström (2004). A commmon origin for aftershocks, foreshocks, and multiplets. *Bull. Seis. Soc. Am. 94*, 88–98.

Felzer, K. R., T. W. Becker, R. E. Abercrombie, Göran Ekström, and J. R. Rice (2002). Triggering of the 1999 $M_W 7.1$ Hector Mine earthquake by aftershocks of the 1992 $M_W 7.3$ Landers earthquake. *J. Geophys. Res. 107*, 2190, doi:10.1029/2001JB000911.

Felzer, K. R. and E. E. Brodsky (2006). Decay of aftershock density with distance indicates triggering by dynamic stress. *Nature 441*, 735–738.

Felzer, K. R. and T. Cao (2008). WGCEP Historical California Earthquake Catalog, Appendix H. *The Uniform California Earthquake Rutpure Forecast (2) (UCERF 2), US Geological Survey Open File Report 2007-1437H*, 127pp.

Glowacka, E., F. A. Neva, G. D. de Cossío, V. Wong, and F. Farfán (2002). Fault slip, seismicity, and deformation in Mexicali Valley, Baja California, Mexico, after the m 7.1 1999 Hector Mine earthquake. *Bull. Seis. Soc. Am. 92*, 1290–1299.

Gomberg, J. (2001). The failure of earthquake failure models. *J. Geophys. Res. 106*, 16253–16263.

Gomberg, J., P. Bodin, and P. A. Reasenberg (2003). Observing earthquakes triggered in the near field by dynamic deformations. *Bull. Seis. Soc. Am. 93*, 118–138.

Gutenberg, B. and C. F. Richter (1944). Frequency of earthquakes in California. *Bull. Seis. Soc. Am. 4*, 185–188.

Helmstetter, A., Y. Y. Kagan, and D. D. Jackson (2006). Comparison of short-term and time-independent earthquake forecast models for Southern California. *Bull. Seis. Soc. Am. 96*, 90–106.

Helmstetter, A. and B. E. Shaw (2006). Relation between stress heterogeneity and aftershock rate in the rate and state model. *J. Geophys. Res. 111*, doi:10.1029/2005JB0040077.

Helmstetter, A. and D. Sornette (2003). Bath's law derived from the Gutenberg-Richter law and from aftershock properties. *Geophys. Res. Lett. 30*, 2069, 10.1029/2003GL018186.

Hill, D. P. (2008). Dynamic stresses, Coulomb failure, and remote triggering. *Bull. Seis. Soc. Am. 98*, 66–92.

Hill, D. P. et al. (1993). Seismicity remotely triggered by the magnitude 7.3 Landers, California, earthquake. *Science 260*, 1617–1623.

Hough, S. E. (2005). Remotely triggered earthquakes following moderate mainshocks (or why California is not falling into the ocean). *Seis. Res. Lett. 76*, 58–66.

Hough, S. E., J. G. Anderson, J. Brune, I. F. Vernon, J. Berger, J. Fletcher, L. Haar, T. Hanks, and L. Baker (1988). Attenuation near Anza, California. *Bull. Seis. Soc. Am. 78*, 672–691.

Hough, S. E. and L. M. Jones (1997). Aftershocks: Are they earthquakes or afterthoughts? *Eos, Trans. Am. Geophys. U. 78*, 505–508.

Kilb, D., J. Gomberg, and P. Bodin (2000). Triggering of earthquake aftershocks by dynamic stresss. *Nature 408*, 570–574.

Kilb, D., V. G. Martynov, and F. L. Vernon (2007). Aftershock detection thresholds as a function of time: Results from the ANZA Seismic Network following the 31 October 2001 m_l 5.1 Anza, California, earthquake. *Bull. Seis. Soc. Am. 97*, doi: 10.1785/0120060116.

Main, I. (2006). A hand on the aftershock trigger. *Nature 441*, 704–705.

Mallman, E. P. and M. D. Zoback (2007). Assessing elastic coulomb stress transfer models using seismicity rates in southern California and southwestern Japan. *J. Geophys. Res. 112*, doi:10.1029/2005JB004076.

Nur, A. and J. R. Booker (1972). Aftershocks caused by pore fluid flow? *Science 175*, 885 – 887.

Ogata, Y. (1988). Statistical models for earthquake occurrence and residual analysis for point processes. *J. Am. Stat. Assoc. 83*, 9–27.

Omori, F. (1894). On the aftershocks of earthquakes. *J. Coll. Sci. Imp. Univ. Tokyo 7*, 111–200.

Parsons, T. (2002). Global Omori law decay of triggered earthquakes: Large aftershocks outside the classical aftershock zone. *J. Geophys. Res. 107*, 2199, doi:10.1029/2001JB000646.

Parsons, T. (2005). A hypothesis for delayed dynamic triggering. *Geophys. Res. Lett. 32*, L04302, doi:10.1029/2004GL021811.

Pollitz, F. F. and M. J. S. Johnston (2006). Direct test of static stress versus dynamic stress triggering of aftershocks. *Geophys. Res. Lett. 33*, doi:10.1029/2006GL026764.

Prejean, S. G., D. P. Hill, E. E. Brodsky, S. E. Hough, M. J. S. Johnston, S. D. Malone, D. H. Oppenheimer, A. M. Pitt, and K. B. Richards-Dinger (2004). Remotely triggerred seismicity on the United States west coast following the m 7.9 Denali fault earthquake. *Bull. Seis. Soc. Am. 94*, S348–S359.

Reasenberg, P. A. and L. M. Jones (1989). Earthquake hazard after a mainshock in California. *Science 243*, 1173–1176.

Richter, C. F. (1958). *Elementary Seismology*. San Francisco: W. F. Freeman.

Scholz, C. H. (1968). Mircrofractures, aftershocks, and seismicity. *Bull. Seis. Soc. Am. 58*, 1117–1130.

Schorlemmer, D., J. Woessner, and C. Bachmann (2006). Probabilistic estimates of monitoring completeness of seismic networks. *Seis. Res. Lett.. 77*, 233.

Silverman, B. W. (1986). *Density Estimation for Statistics and Data Analysis*. New York: Chapman and Hall.

Sornette, A. and D. Sornette (1999). Renormalization of earthquake aftershocks. *26*, 1981–1984.

Steacy, S., J. Gomberg, and M. Cocco (2005). Introduction to special section: Stress transfer, earthquake triggering, and time-dependent seismic hazard. *J. Geophys. Res. 110*, Art. No. B05S01.

Toda, S., R. S. Stein, P. A. Reasenberg, J. H. Dieterich, and A. Yoshida (1998). Stress transfer by the $M_W = 6.9$ Kobe, Japan earthquake: Effect on aftershocks and future earthquake probabilities. *J. Geophys. Res. 103*, 24543–24565.

Utsu, T. (1961). A statistical study on the occurrence of aftershocks. *Geophysical Magazine 30*, 521–605.

Vernon, F. L. (1989). *Analysis of data recorded on the Anza seismic network*. Ph. D. thesis, Scripps Instit. Oceangr., University of California, San Diego.

Walker, K., D. Kilb, and G. Lin (2005). The 2001 and 2005 Anza earthquakes: Aftershock focal mechanisms. In *Southern California Earthquake Center Annual Meeting*.

Wells, D. L. and K. J. Coppersmith (1995). New empirical relationships among magnitude, rupture length, rupture width, rupture area, and surface displacement. *Bull. Seis. Soc. Am. 84*, 974–1002.

West, M., J. J. Sanchez, and S. R. McNutt (2005). Periodically triggered seismicity at Mount Wrangell, Alaska, after the Sumatra earthquake. *Science 308*, 1144–1146.

Tables

Table 1 Direct aftershock parameters for use in the ETAS simualtions. M_{minS} is the magnitude of the smallest earthquake used in the simulations. k, p, and c are modified Omori law parameters (Equation 5).

Figures

Figure 1 The Anza 2005 M_W 5.2 and Yucaipa 2005 M_W 4.7 earthquakes (labeled large stars). The 2001 M_W 5.1 Anza mainshock (square) was within ∼5 km of the 2005 Anza mainshock. Also shown are ANZA network stations (black triangles), SCSN stations (grey triangles) and 154 larger events in the region, M> 4.0, from the ANZA catalog that occurred during years 1982 to 2005 (grey circles)

Figure 2 Map of the first two days of the aftershocks in the 2001 and 2005 Anza sequences, recorded by Anza Seismic Network stations (inverted triangles). To illustrate that the sequences would appear spatially much smaller if only larger earthquakes had been observed, we present data restricted to various magnitude ranges (indicated in plot titles). For reference, a 40 km radius circle is drawn around each mainshock epicenter. (A) Map of the 198 recorded $M \geq 1.0$ earthquakes in the Anza 2001 sequence. (B) Map of the 387 recorded $M \geq 0.5$ earthquakes in the Anza 2005 sequence. (C) Map of the 15 recorded $M \geq 2.0$ earthquakes in the Anza 2001 sequence. (D) Map of the 25 recorded $M \geq 2.0$ earthquakes in the Anza 2005 sequence. For comparison, the squares in each figure show seismicity in the 2 days before each mainshock, down to the same magnitude cutoffs. There was very little seismicity in the two days preceding the 2005 mainshock.

Figure 3 Temporal examination of earthquake magnitudes (points) recorded by the SCSN and ANZA networks. Data is restricted to the region: 33.3° < lat < 33.75°, -117.25° < lon < -116.25°. This region was chosen to be as big as possible while at the same time avoiding the large signature of the M_W7.3 1992 Landers earthquake and the M_W7.1 1999 Hector Mine earthquake. Only recently have small magnitude earthquakes been routinely recorded and cataloged, as indicated by the decrease in the median earthquake magnitude for a moving window of 250 consecutive events (non-linear grey line). For reference, the shaded region encompasses magnitudes below 0.5. (a) SCSN data (35,293 earthquakes). (b) ANZA data (23,922 earthquakes.

Figure 4 Comparison of earthquake magnitudes for common event pairs in the ANZA and SCSN catalogs.

Data consists of 350 and 531 earthquake pairs in the 2001 and 2005 sequences, respectively. The mean difference in magnitudes for the 2001 sequence is 0.6±0.3 and for the 2005 sequence is 0.5±0.3. (a) Magnitude histogram of data from the ANZA network catalog for the 2001 sequence. (b) as in (a) but for the SCSN catalog. (c) Magnitude histogram of data from the ANZA network catalog for the 2005 sequences. (d) As in (c) but for the SCSN catalog.

Figure 5 Schematic of measuring linear aftershock density with the nearest neighbor technique, with k (number of earthquakes/group) set equal to 1. (A) A mainshock and ten aftershocks are plotted in map view. (B) The aftershocks are depicted on a line where their position is dictated by their distance from the mainshock. As an example, we calculate linear density at the position of the eighth aftershock. Since the earthquake group size = 1, the center point of the measurement, or r_c, is at the position of this aftershock. Linear density at r_c is given by k/r_8 or $1/r_8$, where r_8 reaches from the midpoint between aftershocks 7 and 8 to the midpoint between aftershocks 8 and 9.

Figure 6 Cumulative magnitude frequency plots of the first two days of aftershocks in the 2001 and 2005 Anza sequences, used to roughly estimate sequence completeness thresholds. (A) 2001 Anza aftershocks recorded by the Anza network (data from 499 earthquakes). (B) 2005 Anza aftershocks recorded by the Anza network (data from 1351 earthquakes). (C) 2001 Anza aftershocks catalogued by the SCSN network (data from 421 earthquakes). (D) 2005 Anza aftershocks catalogued by the SCSN network (data from 593 earthquakes.

Figure 7 Aftershock hypocentral distance from the mainshock versus aftershock density, restricted to $M_L \geq$ 0.5 ANZA network data (open circles). Aftershock data that locate between 4 and 40 km from the mainshock are used to determine a best fit distance-to-density relationship (dashed grey line) and associated decay values. These lines are then extrapolated to 1 km distance for visual comparison. At very close distances we expect the decay curve to flatten because of earthquake mislocation, inaccuracies of the modeled mainshock fault plane, and near field catalog incompleteness (e.g., see Felzer and Brodsky (2006)) (A) The 2001 Anza sequence. The 68 aftershocks in the distance ranges 4 to 40 km has a best fit power law (dashed line) that has an exponent of -1.76. (B) The 2005 Anza sequence. As in (A) using 49 aftershocks in the distance ranges 4 to 40 km, produce a best fit power law (dashed line) that has an exponent of -1.85. The expected average decay exponent for normal aftershock sequences in southern California is -1.37, with variation expected from sequence to sequence as a function of local fault geometry.

Figure 8 Simulation of the first two days of aftershocks in the 2001 and 2005 Anza sequences. These maps can be compared with the true data in Figure 2. For spatial reference, a 40 km radius circle is drawn around each mainshock epicenter. These maps illustrate, even in the simulations, how much smaller the sequences appear when only aftershocks larger than magnitude 2, the usual completeness threshold for Southern California aftershock sequences, are plotted. Data from simulations of: (A) The Anza 2001 sequence for 348 $M \geq 1.0$ earthquakes; and (B) The Anza 2005 sequence for 1585 $M \geq 0.5$ for earthquakes. (C) As in (A) but including only the 49 $M \geq 2.0$ earthquakes; and (D) As in (B) but but including only the 40 $M \geq 2.0$ earthquakes. While only single simulated sequences are plotted here, the range of aftershock densities at different distances from a total of 500 ETAS simulations are plotted in Figure 9, where they are shown to agree with the real data.

Figure 9 Expected (solid symbols) and observed (open symbols) number of aftershocks (restricted to $M_L \geq 0.5$) in the first two days of each sequence as a function of hypocentral distance from the mainshock fault plane for the: (A) 2001 Anza sequence; and (B) 2005 Anza sequence. The expected number of aftershocks in distance bins that range between 10 and 40 km are extrapolated using the number of observed aftershocks between 4 and 10 km and Equation 1. Error bars give the 98% confidence range of the modeled values, estimated from 500 ETAS simulations with data sets of this size. The observed number of aftershocks from the Anza network catalog (squares) and the observed number in the SCSN catalog (triangles) primarily fall within the modeled error bars. Because there is a 0.5 magnitude unit offset in the Anza and SCSN catalogs, for the SCSN data we only measure $M \geq 1.0$ earthquakes.

M_{minS}	k	p	c
0.5	0.0068	1.34	0.09

Table 1: Direct aftershock parameters for use in the ETAS simualtions. M_{minS} is the magnitude of the smallest earthquake used in the simulations. k, p, and c are modified Omori law parameters (Equation 5).

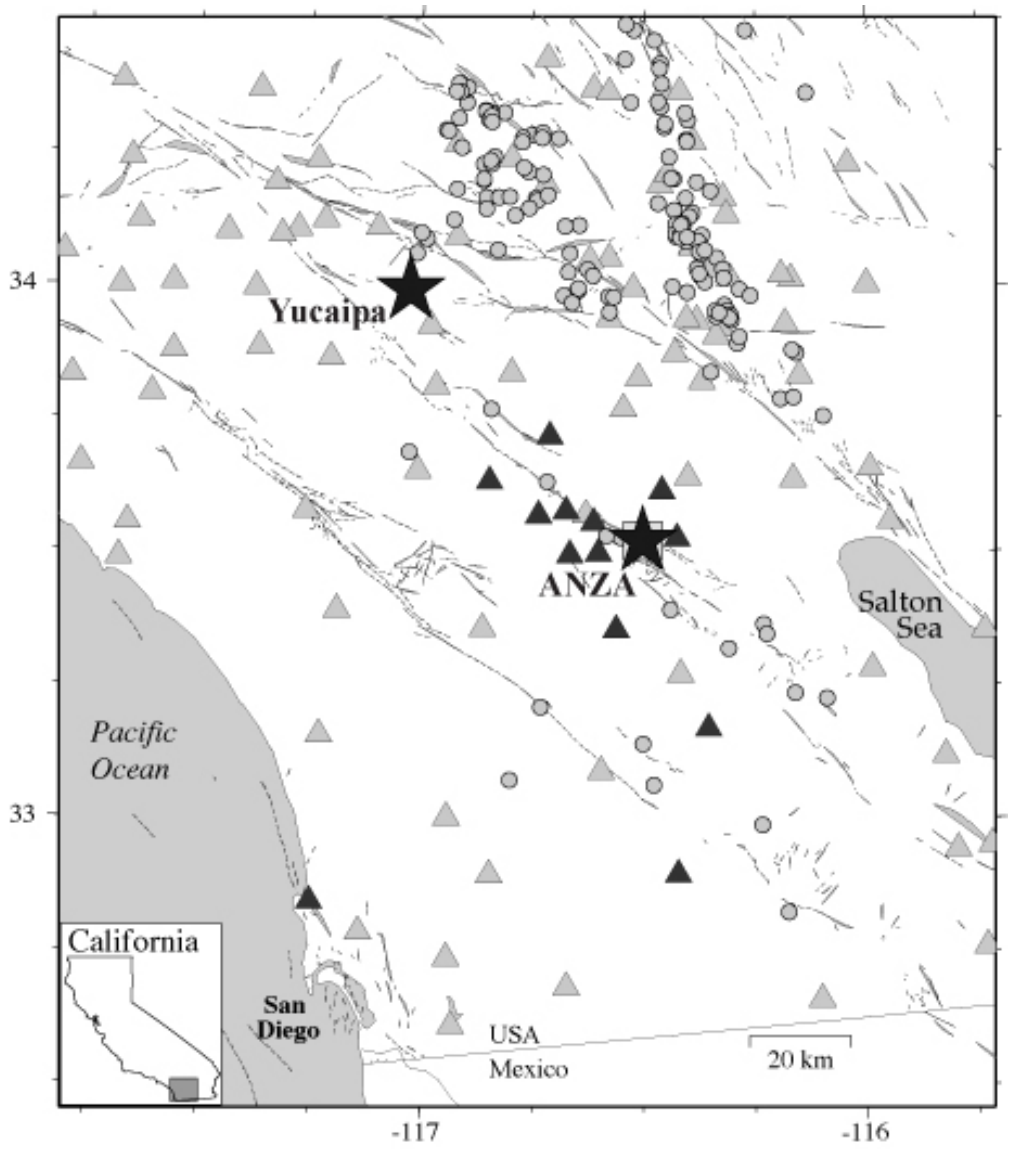

Figure 1: The Anza 2005 M_W 5.2 and Yucaipa 2005 M_W 4.7 earthquakes (labeled large stars). The 2001 M_W 5.1 Anza mainshock (square) was within ∼5 km of the 2005 Anza mainshock. Also shown are ANZA network stations (black triangles), SCSN stations (grey triangles) and 154 larger events in the region, M> 4.0, from the ANZA catalog that occurred during years 1982 to 2005 (grey circles).

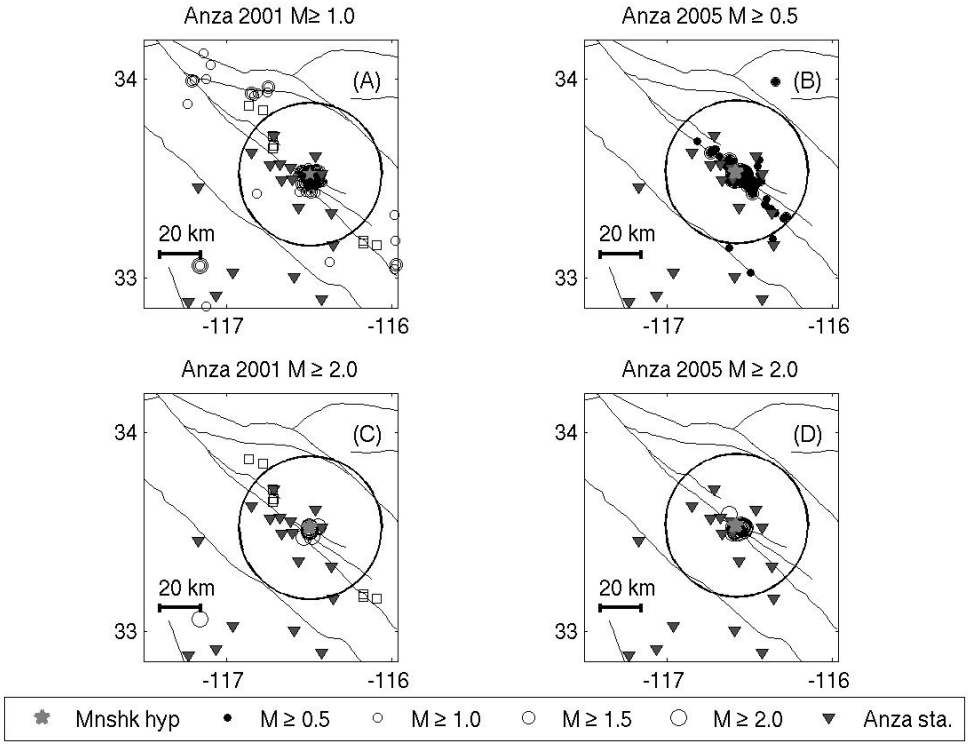

Figure 2: Map of the first two days of the aftershocks in the 2001 and 2005 Anza sequences, recorded by Anza Seismic Network stations (inverted triangles). To illustrate that the sequences would appear spatially much smaller if only larger earthquakes had been observed, we present data restricted to various magnitude ranges (indicated in plot titles). For reference, a 40 km radius circle is drawn around each mainshock epicenter. (A) Map of the 198 recorded $M \geq 1.0$ earthquakes in the Anza 2001 sequence. (B) Map of the 387 recorded $M \geq 0.5$ earthquakes in the Anza 2005 sequence. (C) Map of the 15 recorded $M \geq 2.0$ earthquakes in the Anza 2001 sequence. (D) Map of the 25 recorded $M \geq 2.0$ earthquakes in the Anza 2005 sequence. For comparison, the squares in each figure show seismicity in the 2 days before each mainshock, down to the same magnitude cutoffs. There was very little seismicity in the two days preceding the 2005 mainshock.

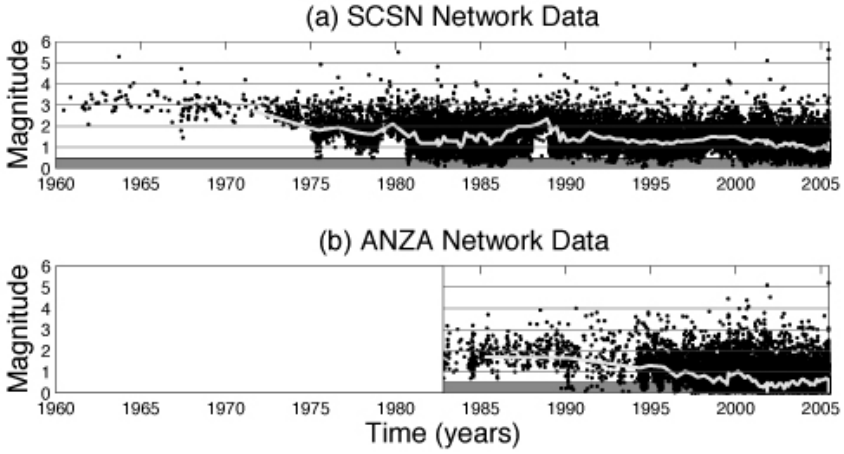

Figure 3: Temporal examination of earthquake magnitudes (points) recorded by the SCSN and ANZA networks. Data is restricted to the region: 33.3° < lat < 33.75°, -117.25° < lon < -116.25°. This region was chosen to be as big as possible while at the same time avoiding the large signature of the $M_W 7.3$ 1992 Landers earthquake and the $M_W 7.1$ 1999 Hector Mine earthquake. Only recently have small magnitude earthquakes been routinely recorded and cataloged, as indicated by the decrease in the median earthquake magnitude for a moving window of 250 consecutive events (non-linear grey line). For reference, the shaded region encompasses magnitudes below 0.5. (a) SCSN data (35,293 earthquakes). (b) ANZA data (23,922 earthquakes).

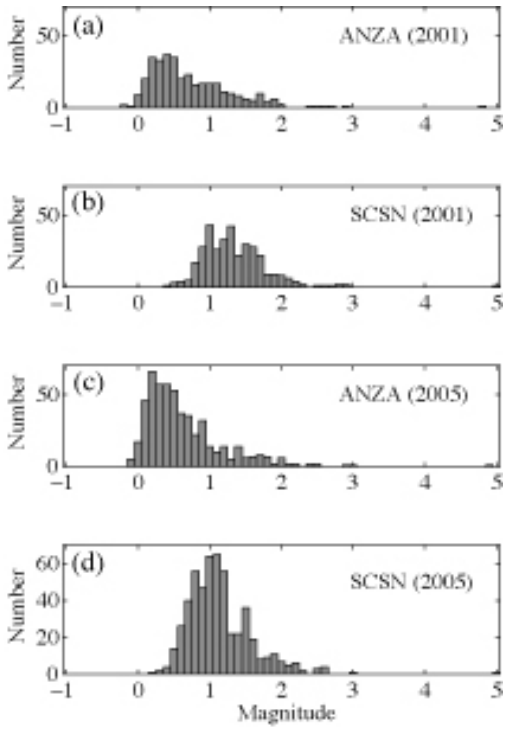

Figure 4: Comparison of earthquake magnitudes for common event pairs in the ANZA and SCSN catalogs. Data consists of 350 and 531 earthquake pairs in the 2001 and 2005 sequences, respectively. The mean difference in magnitudes for the 2001 sequence is 0.6 ± 0.3 and for the 2005 sequence is 0.5 ± 0.3. (a) Magnitude histogram of data from the ANZA network catalog for the 2001 sequence. (b) as in (a) but for the SCSN catalog. (c) Magnitude histogram of data from the ANZA network catalog for the 2005 sequences. (d) As in (c) but for the SCSN catalog.

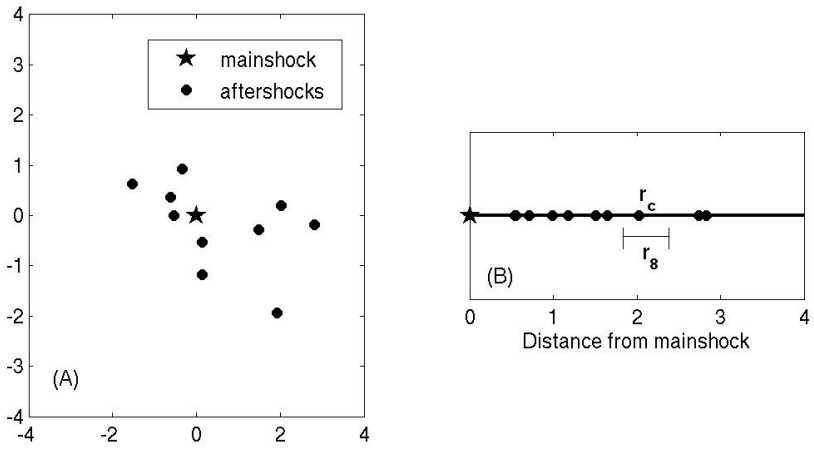

Figure 5: Schematic of measuring linear aftershock density with the nearest neighbor technique, with k (number of earthquakes/group) set equal to 1. (A) A mainshock and ten aftershocks are plotted in map view. (B) The aftershocks are depicted on a line where their position is dictated by their distance from the mainshock. As an example, we calculate linear density at the position of the eighth aftershock. Since the earthquake group size = 1, the center point of the measurement, or r_c, is at the position of this aftershock. Linear density at r_c is given by k/r_8 or $1/r_8$, where r_8 reaches from the midpoint between aftershocks 7 and 8 to the midpoint between aftershocks 8 and 9.

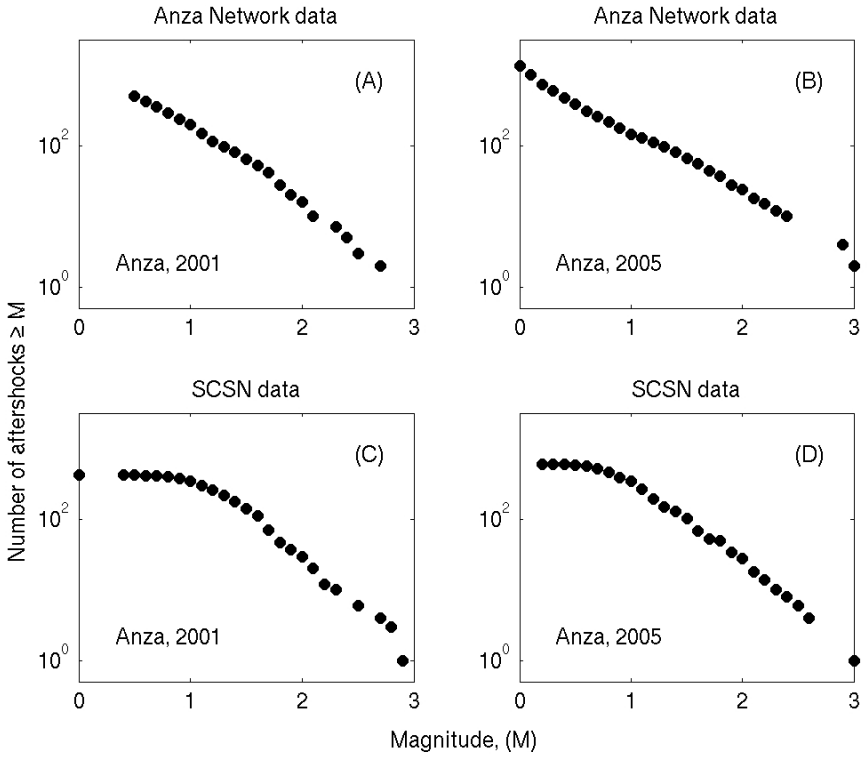

Figure 6: Cumulative magnitude frequency plots of the first two days of aftershocks in the 2001 and 2005 Anza sequences, used to roughly estimate sequence completeness thresholds. (A) 2001 Anza aftershocks recorded by the Anza network (data from 499 earthquakes). (B) 2005 Anza aftershocks recorded by the Anza network (data from 1351 earthquakes). (C) 2001 Anza aftershocks catalogued by the SCSN network (data from 421 earthquakes). (D) 2005 Anza aftershocks catalogued by the SCSN network (data from 593 earthquakes).

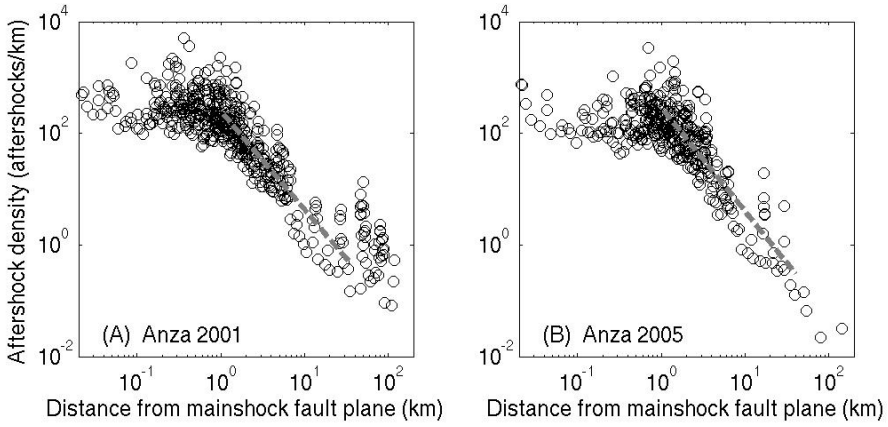

Figure 7: Aftershock hypocentral distance from the mainshock versus aftershock density, restricted to $M_L \geq$ 0.5 ANZA network data (open circles). Aftershock data that locate between 4 and 40 km from the mainshock are used to determine a best fit distance-to-density relationship (dashed grey line) and associated decay values. These lines are then extrapolated to 1 km distance for visual comparison. At very close distances we expect the decay curve to flatten because of earthquake mislocation, inaccuracies of the modeled mainshock fault plane, and near field catalog incompleteness (e.g., see Felzer and Brodsky (2006)) (A) The 2001 Anza sequence. The 68 aftershocks in the distance ranges 4 to 40 km has a best fit power law (dashed line) that has an exponent of -1.76. (B) The 2005 Anza sequence. As in (A) using 49 aftershocks in the distance ranges 4 to 40 km, produce a best fit power law (dashed line) that has an exponent of -1.85. The expected average decay exponent for normal aftershock sequences in southern California is -1.37, with variation expected from sequence to sequence as a function of local fault geometry.

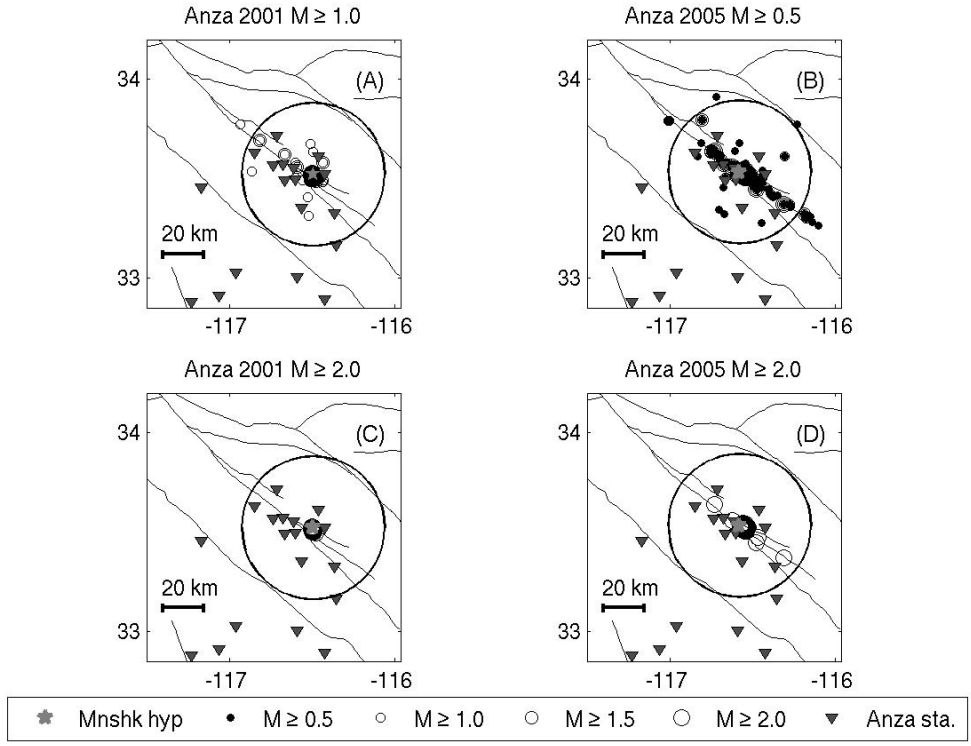

Figure 8: Simulation of the first two days of aftershocks in the 2001 and 2005 Anza sequences. These maps can be compared with the true data in Figure 2. For spatial reference, a 40 km radius circle is drawn around each mainshock epicenter. These maps illustrate, even in the simulations, how much smaller the sequences appear when only aftershocks larger than magnitude 2, the usual completeness threshold for Southern California aftershock sequences, are plotted. Data from simulations of: (A) The Anza 2001 sequence for 348 $M \geq 1.0$ earthquakes; and (B) The Anza 2005 sequence for 1585 $M \geq 0.5$ for earthquakes. (C) As in (A) but including only the 49 $M \geq 2.0$ earthquakes; and (D) As in (B) but but including only the 40 $M \geq 2.0$ earthquakes. While only single simulated sequences are plotted here, the range of aftershock densities at different distances from a total of 500 ETAS simulations are plotted in Figure 9, where they are shown to agree with the real data.

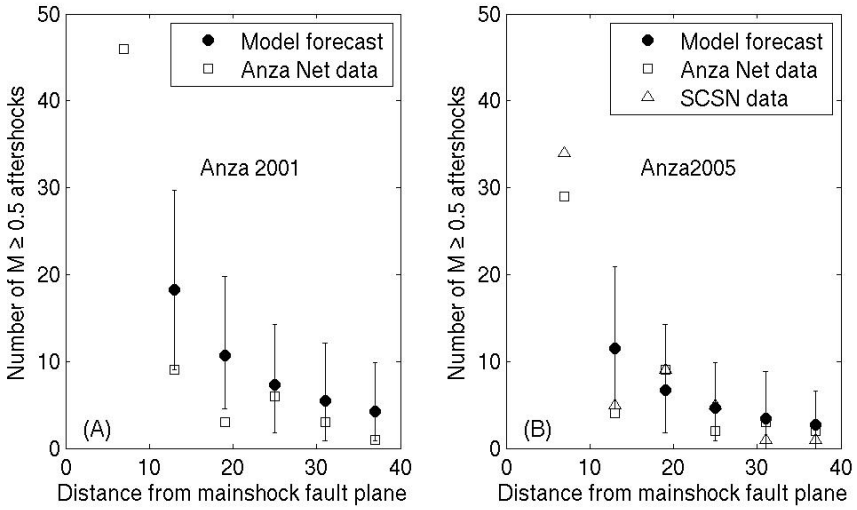

Figure 9: Expected (solid symbols) and observed (open symbols) number of aftershocks (restricted to $M_L \geq 0.5$) in the first two days of each sequence as a function of hypocentral distance from the mainshock fault plane for the: (A) 2001 Anza sequence; and (B) 2005 Anza sequence. The expected number of aftershocks in distance bins that range between 10 and 40 km are extrapolated using the number of observed aftershocks between 4 and 10 km and Equation 1. Error bars give the 98% confidence range of the modeled values, estimated from 500 ETAS simulations with data sets of this size. The observed number of aftershocks from the Anza network catalog (squares) and the observed number in the SCSN catalog (triangles) primarily fall within the modeled error bars. Because there is a 0.5 magnitude unit offset in the Anza and SCSN catalogs, for the SCSN data we only measure $M \geq 1.0$ earthquakes.